THE JOURNAL OF PHYSICAL CHEMISTRY B LETTERS

2007, *111,* 7469−7472
Published on Web 06/14/2007

Coherent Carbon Cryogel−Ammonia Borane Nanocomposites for H_2 Storage

Aaron Feaver,[†] Saghar Sepehri,[†] Patrick Shamberger,[†] Ashley Stowe,[‡] Tom Autrey,[‡] and Guozhong Cao*,[†]

Materials Science & Engineering, University of Washington, 302 Roberts Hall, Box 352120, Seattle, Washington 98195, and Pacific Northwest National Laboratory (PNNL), 902 Battelle Boulevard, Box 999, Richland, Washington 99352

Received: March 28, 2007; In Final Form: May 24, 2007

Coherent carbon cryogel−ammonia borane (C−AB) nanocomposites were synthesized, and improved H_2 storage properties are reported. Porous carbon cryogels were impregnated with AB in tetrahydrofuran solution at 25 °C under argon; 30% of the carbon cryogel pore volume was filled to produce a 24 wt % C−AB nanocomposite. Nitrogen sorption isotherms, X-ray diffraction, differential scanning calorimetry, differential thermal/thermal gravimetric analyses, mass spectrometry, and ^{11}B NMR were used to characterize the coherent C−AB nanocomposites. Findings include a merged two-step hydrogen release reaction with an appreciable reduction in the dehydrogenation temperature to <90 °C as well as the suppression of borazine release. The possible nanosize effects on the H_2 storage properties are discussed.

Introduction

Hydrogen fuel offers many potential advantages over fossil fuels, such as generation from renewable sources, elimination of pollution through zero-point source emissions, and compatibility with fuel cells.[1,2] Recent research efforts have focused on solving the problems of H_2 generation and storage.[3,4] Among the possible H_2 storage techniques and materials, metal hydrides or complex hydrides have the potential to store hydrogen at the necessary gravimetric and volumetric densities at ambient temperatures and pressures.[5,6] However, hydrides generally suffer from at least one of the following: high dehydrogenation temperature, poor reversibility, or slow kinetics.[7] Nanostructured hydrides may offer a solution because they often exhibit significantly different physical, chemical, and thermodynamic characteristics from bulk materials.[8] Experimental results on nanoscale hydrides have clearly demonstrated improvements in the reaction kinetics or thermodynamics of hydrogenation or dehydrogenation,[8] though the exact mechanism for the improved properties often remains unknown. For example, nanocomposites comprised of ammonia borane (AB) and mesoporous silica have demonstrated a reduction in dehydrogenation temperature and a significant improvement in kinetics.[9] However, silica is relatively heavy and has a poor thermal conductivity. The coherent carbon cryogel−AB (C−AB) nanocomposites reported in this paper, as schematically illustrated in Figure 1, offer a number of potential benefits; a percolated carbon network serves as a thermal conduction pathway, adjustable pore diameter provides size confinement for hydride particles, and the carbon matrix supports the powder mechanically, with minimal added weight due to low atomic mass of carbon. Carbon cryogels also offer many relevant tunable properties such as pore volume, pore size, surface area, and surface chemistry for possible catalytic effects. In addition, the micropore volume in carbon cryogels may be used to store extra H_2 through surface adsorption under an appropriate condition. This letter presents experimental results that show the substantial benefits of one type of C−AB nanocomposite, but further improvement is expected due to the tunability of the carbon cryogel matrix material.

Experimental Section

Carbon cryogels are derived from resorcinol formaldehyde hydrogels by freeze drying and pyrolyzing at elevated temperatures in N_2, and their porous structure can be readily tuned by controlling sol−gel parameters and pyrolysis conditions.[10] In the present study, carbon cryogels with a surface area of 300 m^2/g, a pore volume of 0.70 cm^3/g (57% open porosity), and pores ranging from 2 to 20 nm in diameter have been used to incorporate up to 24 wt % of AB by soaking carbon cryogels in a solution of tetrahydrofuran (THF) and AB under argon at room temperature. The excess AB on the surface was carefully washed off, and the nanocomposites were dried under vacuum and stored in argon at room temperature prior to further analyses.

Results and Discussion

X-ray diffraction analysis (Figure 2) reveals that the crystal structure of AB, peaks at 23.8 (110), 24.4 (101), 34.0 (200), 35.6 (002), 42.4 (121), and 43.3° (112), in the nanocomposites over a background amorphous signal from the carbon cryogel is in agreement with the literature (JCPDS Card No. 13-0292).[11,12] However, it is evident from the most prominent peaks between $2\theta = 23$ and 25° that a clear splitting of the peaks and a small shift has occurred. Such changes in the XRD peaks can arise from the stress exerted on the AB crystal by the cryogel

* To whom correspondence should be addressed. E-mail: gzcao@u.washington.edu.
[†] University of Washington.
[‡] Pacific Northwest National Laboratory.

10.1021/jp072448t CCC: $37.00

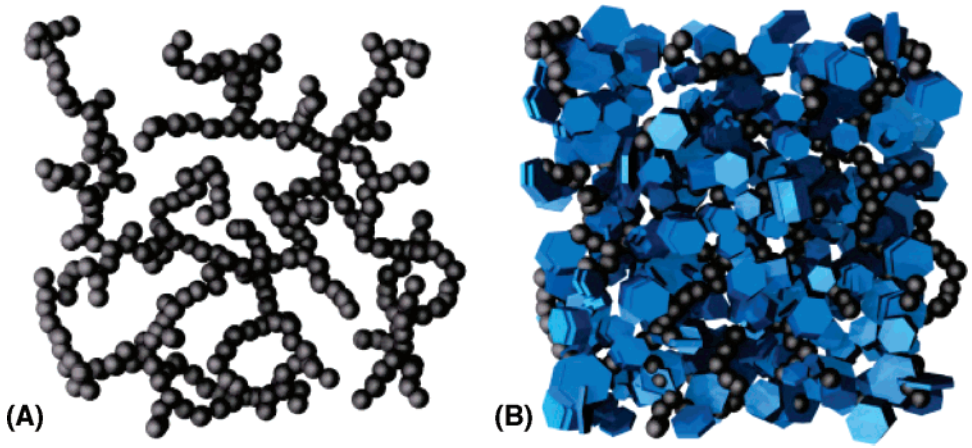

Figure 1. Schematic of (A) an unmodified carbon cryogel and (B) a C−AB nanocomposite.

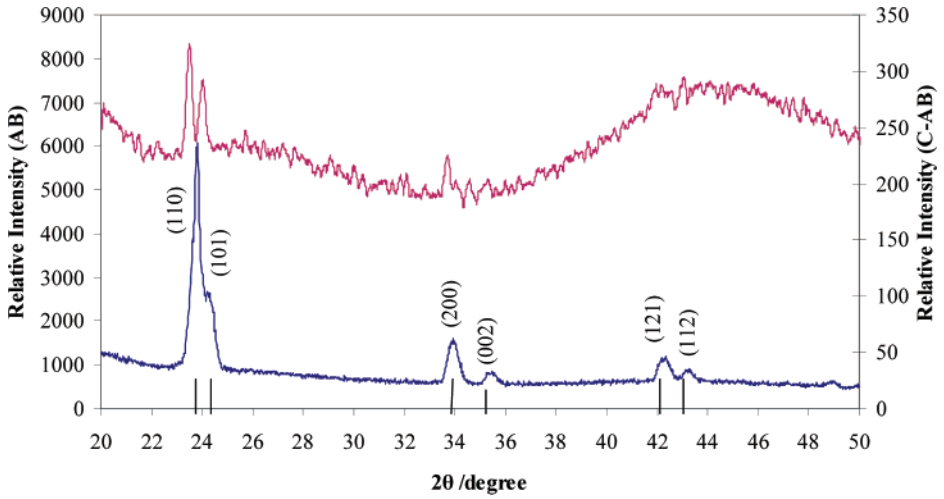

Figure 2. XRD pattern of a powdered C−AB nanocomposite (above) and neat AB (below). The XRD for C−AB nanocomposite shows AB peaks behind an amorphous carbon cryogel hump. The (110)−(101) peaks for AB are split in C−AB, possibly as a result of the stress from the cryogel matrix on the AB crystals.

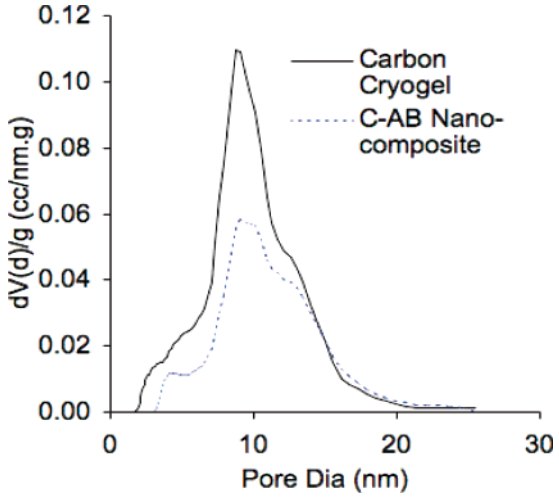

Figure 3. Pore size distribution showing the effect of loading with AB for a 24 wt % C−AB nanocomposite.

matrix.[13] Nitrogen sorption isotherm analyses demonstrate an appreciable reduction in both pore volume (∼30% reduction) and surface area (∼50%) upon the incorporation of AB, as shown in Figure 3. Analysis of several samples at different loading percentages shows that the reduction in pore volume and surface area corresponds well to the amount of AB incorporated. However, it is interesting to note that there is no detectable reduction in pore diameter, and the overall pore size distribution remains almost unchanged, regardless of the amount of AB incorporated into the carbon cryogels. The reduction of both pore volume and surface area are explained by the likelihood that some pores are either completely or partially filled with AB. However, the lack of pore diameter reduction indicates that tiny pockets of the cryogel remain unfilled, while the overall loading is even. This notion is further supported by differential scanning calorimetry (DSC) results that showed nearly identical thermal response from various parts of an ∼1 cm^3 C−AB nanocomposite, thus proving that the AB is not simply coated onto the outside or subsurface layer of the cryogel. Improvement in the process of AB incorporation is underway to achieve higher loading and a better understanding of the process. AB loading of 1:1 AB/carbon by weight has already been achieved, and a detailed characterization will be reported in future publications.

Figure 4 compares the dehydrogenation properties of pure AB and the C−AB nanocomposite (24 wt % AB) measured by simultaneous differential thermal analysis (DTA) and mass spectrometry (MS) with a heating rate of 1 °C/min. The first noticeable difference is that neat AB has a DTA curve (Figure 4A) rather different from that of the nanocomposite. Neat AB generates an endothermic dip at ∼105 °C and two exothermic maxima at ∼110 and ∼150 °C, whereas the nanocomposite shows only an exothermic peak at ∼90 °C. MS results also show that the nanocomposite releases hydrogen at much lower

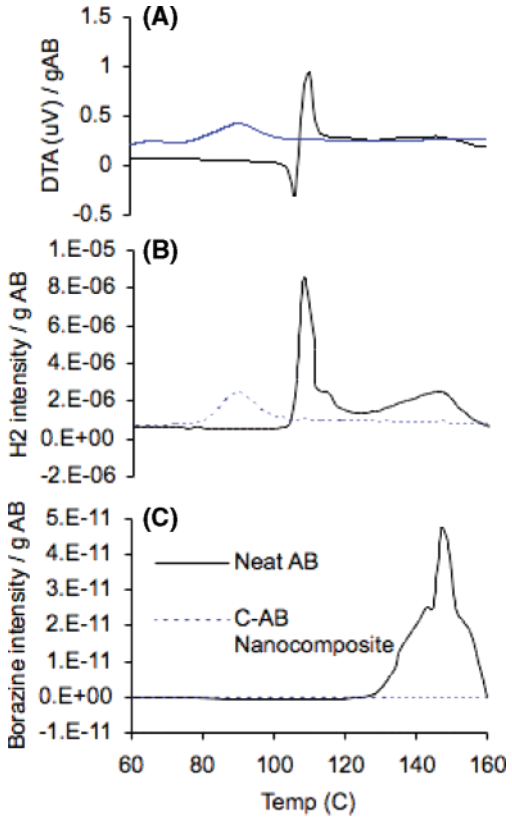

Figure 4. (A) DTA results of the C−AB nanocomposite and neat AB with a heating rate of 1 °C/min; (B) H_2 MS readings showing the H_2 release at ∼90 °C in a C−AB nanocomposite and at 110 and 150 °C in neat AB; and (C) the borazine MS readings showing no release of borazine from the C−AB nanocomposite.

temperatures, with a broad peak centered at ∼90 °C, while neat AB has a sharp peak of hydrogen release at ∼110 °C followed by a second broad peak at ∼150 °C. Additionally, MS demonstrates that the C−AB nanocomposite suppresses the formation and/or release of borazine, as can be seen in Figure 4C. Borazine is an undesirable byproduct of AB dehydrogenation that will foul a fuel cell membrane and eventually render it unusable. Neat AB releases a significant amount of borazine upon heating to higher temperatures, as is also reported in the literature.[14]

The DTA and MS results of neat AB are in good agreement with the literature[15,16] and are explained below. At this moderate heating rate, the endothermic dip is attributed to the melting phase transition immediately followed by dehydrogenation, with a peak at ∼110 °C corresponding to 1 mol or 6.5 wt % of H_2 released from AB.[12] At higher temperatures (∼150 °C), one more equivalent of hydrogen is released presumably from the polymeric NH_2BH_2 product of the first reaction.[17] These two reactions release a total of 13 wt % of H_2 if the reactions are complete, as we have observed in volumetric measurements of neat AB dehydrogenation (not shown here). The DTA and MS results from nanocomposites are significantly different. The dehydrogenation started at <80 °C and peaked at ∼90 °C, and no further dehydrogenation at temperatures between 110 and 160 °C was observed. It is also noticed that the C−AB dehydrogenation peak is significantly broader than the dehydrogenation peak of neat AB. Volumetric measurements have shown that an approximately equivalent 9 wt % of hydrogen from AB is released from the nanocomposites. DSC results demonstrate that the dehydrogenation reaction is concurrent with a −120 kJ/mol exothermic reaction that is significantly more exothermic than neat AB at −21 kJ/mol.[9]

There are several possible explanations for the observed differences in the dehydrogenation of the nanocomposite. One is the size effect. Considering that pores in these carbon cryogels range from 2 to 20 nm in diameter and the full distribution of pores has been reduced in volume, the AB particles in the composite must be smaller than the pore size. Other systems with diameters in the nanometer range or smaller possess a huge relative surface area and thus surface energy and, consequently, often have a significantly lowered phase transition temperature.[18,19] It is quite possible that the dehydrogenation temperature decreases with the reducing diameter of AB crystals. Another possibility is that the inner surface of the carbon cryogel with a lot of dangling bonds, having intimate contact with the AB, exerts catalytic influences on the dehydrogenation of AB or at least serves as the initial nucleation site for the phase transition of AB leading to hydrogen release. Both proposed mechanisms can also explain the broadened dehydrogenation peaks in the C−AB nanocomposite. AB nanoparticles inside carbon cryogel are expected to have a size distribution, and different sized nanoparticles may have different dehydrogenation temperatures based on the surface or interface area. The above explanation is partly corroborated by the reduced hydrogenation temperature of mesoporous silica−AB nanocomposites,[9] although silica and carbon are obviously different materials. Mesoporous silica has a pore size of 7.5 nm, and mesoporous silica−AB nanocomposites showed a dehydrogenation temperature of ∼98 °C. Our further experiments have revealed that the dehydrogenation temperature decreases further as the pores of carbon cryogels get smaller. For example, carbon cryogels with a pore size maximum at 5 nm result in a peak dehydrogenation temperature of 85 °C when incorporated with AB. Further experiments to establish the relationship between dehydrogenation temperature and pore size are underway and will be reported separately later.

The release of 9 wt % of hydrogen from nanocomposites has also been further investigated. ^{11}B NMR has clearly demonstrated that the AB inside of the carbon cryogels undergoes both stages of the dehydrogenation reaction described above, but at temperatures as low as 60 °C. In addition, in situ NMR studies on the kinetics of this reaction have shown that the rates are substantially faster than even those of the silica−AB composites. The two-stage reaction helps explain the 9 wt % of hydrogen release but does not account for all of the additional energy released by this material, and theoretically, the AB should release 13 wt %. However, when considering the low dehydrogenation temperatures, it is likely that some hydrogen may be lost during the fabrication of nanocomposites at room temperature, thus accounting for 13 wt % being reduced to 9 wt %. Studies have found that carboxyl groups are the most common surface groups in carbon aerogels (akin to carbon cryogels).[20] We have noticed that AB will react at much lower temperatures in acidic environments, as has been observed with borohydride.[21] The carboxyl acidic surface of the carbon cryogel may be resulting in partial dehydrogenation before H_2 release tests can be performed. Release of gas during the fabrication of nanocomposites has indeed been observed in our experiments. Passivation or removal of surface carboxyl groups from carbon cryogels would prevent such undesired dehydrogenation.

Conclusions

The coherent carbon cryogel−AB nanocomposites release two hydrogen molecules in a two-in-one reaction at significantly reduced dehydrogenation temperatures and pose the possibility of tuning by controlling the pore size of carbon cryogels. The differences from the bulk material are attributed to the size-

dependent surface energy of AB confined inside of the nanoscale pores of carbon cryogels as well as a possible catalytic effect from the carbon−AB interface. A hydrogen release of 9 wt % from AB was obtained, and the formation and/or release of borazine was suppressed. It is demonstrated that a 13 wt % hydrogen release from AB in the form of a nanocomposite at low temperatures is a reasonable target. Overall hydrogen storage capacity will be dependent on both AB loading and the number of hydrogen molecules released from each AB molecule.

Acknowledgment. This work is support by the NSF (DMR-0605159), WTC, and EnerG2 LLC as well as the DoE Center of Excellence in Chemical Hydrogen Storage funded by the DOE H_2 Program. A.F. is also grateful for the NSF-IGERT and the Joint Institute of Nanoscience fellowships. Part of this research was performed in the William R. Wiley Environmental Molecular Sciences Laboratory located at the Pacific Northwest National Laboratory which is operated by Battelle for the U.S. Department of Energy.

References and Notes

(1) Solomon, B. D.; Banerjee, A. *Energy Policy* **2006**, *34*, 781.
(2) Granovski, M.; Dincer, I.; Rosen, M. *Int. J. Hydrogen Energy* **2006**, *31*, 337.
(3) Nikbin, D. *Fuel Cell Rev.* **2006**, *3*, 15.
(4) Bai, Y.; Wu, C.; Wu, F.; Yi, B. *Mater. Lett.* **2006**, *60*, 2236.
(5) Kelly, M.; Briggs, A. 24th Annual International Telecommuncations Energy Conference, Montreal, Quebec, Canada, 2002.
(6) Dedrick, D. E.; Kanouff, M. P.; Replogle, B. C.; Gross, K. L. *J. Alloy Compd.* **2005**, *389*, 299.
(7) Zutell, A. *Mater. Today* **2003**, *6*, 24.
(8) Seayad, A. M.; Antonelli, D. M. *Adv. Mater.* **2004**, *16*, 765.
(9) Gutowska, A.; Liyu, L.; Shin, Y.; Chongmin, M.; Wang, X.; Li, S.; Linehan, J.; Smith, S.; Kay, B. D.; Schmid, B.; Shaw, W.; Gutowski, M.; Autrey, T. *Angew. Chem., Int. Ed.* **2005**, *44*, 3578.
(10) Feaver, A.; Cao, G. Z. *Carbon* **2006**, *44*, 590.
(11) DeBenedetto, S.; Carewska, M.; Cento, C.; Gislon, P.; Pasquali, M.; Scaccia, S.; Prosini, P. P. *Thermochim. Acta* **2006**, *441*, 184.
(12) Stowe, A. C.; Shaw, W. J.; Linehan, J. C.; Schmid, B.; Autrey, T. *Phys. Chem. Chem. Phys.* **2007**, *9*, 1831.
(13) Wu, X. L.; Tong, S.; Liu, X. N.; Bao, X. M.; Jiang, S. S.; Feng, D. *Appl. Phys. Lett.* **1997**, *70*, 838.
(14) Wolf, G.; Baumann, J.; Baitalow, F.; Hoffmann, F. P. *Thermochim. Acta* **2000**, *343*, 19.
(15) Baitalow, F.; Baumann, J.; Wolf, G.; Jaenicke-RoBler, K.; Leitner, G. *Thermochim. Acta* **2002**, *391*, 159.
(16) Komm, R.; Geanangel, R. A.; Liepins, R. *Inorg. Chem.* **1983**, *22*, 1685.
(17) Baumann, J.; Baitalow, F.; Wolf, G. *Thermochim. Acta* **2005**, *430*, 9.
(18) Sasaki, K.; Saka, H. *Philos. Mag. A* **1991**, *63*, 1207.
(19) Ohashi, T.; Kuroda, K.; Sasa, H. *Philos. Mag. B* **1992**, *65*, 1041.
(20) Goel, J.; Kadirvelu, K.; Rajagopal, C.; Garg, V. K. *J. Chem. Technol. Biotechnol.* **2005**, *80*, 469.
(21) Levine, L. A.; Kreevoy, M. K. *J. Am. Chem. Soc.* **1972**, *94*, 3346.